2015

Absorption enhancement in double-sided nanocone hole arrays for solar cells

Xu Zhang
University of Wollongong, xuzhang@uow.edu.au

Yanguang Yu
University of Wollongong, yanguang@uow.edu.au

Jiangtao Xi
University of Wollongong, jiangtao@uow.edu.au

Yile Wang
Zhengzhou University

Xiao-Hong Sun
Zhengzhou University

Publication Details

X. Zhang, Y. Yu, J. Xi, Y. Wang & X. Sun, "Absorption enhancement in double-sided nanocone hole arrays for solar cells," Journal of Optics, vol. 17, (7) pp. 1-6, 2015.

Absorption enhancement in double-sided nanocone hole arrays for solar cells

Abstract
Enhancing light absorption in thin-film silicon solar cells is important for improving light harvesting efficiency and reducing manufacture cost. In this paper, we introduce a double-sided nanocone hole (NCH) array structure for solar cells by extending a model suggested by Wang et al (2012 Nano Lett. 12 1616). The top-sided NCH structure is mainly used for increasing the antireflection of incident light, and the bottom-sided NCH structure for enhancing light trapping in the near-infrared spectrum. The theoretical analysis is performed on the proposed structure, from which the optimal geometric parameters of the structure are determined. The performance analysis shows that the proposed optimized double-sided NCH structure can yield a short-circuit current of 31.9 mA cm^{-2} with equivalent thickness of 1 μm, which is 12% and 190% higher than that of the top-sided NCH and planar film counterparts, respectively.

Keywords
enhancement, double, sided, absorption, nanocone, cells, hole, arrays, solar

Disciplines
Engineering | Science and Technology Studies

Publication Details
X. Zhang, Y. Yu, J. Xi, Y. Wang & X. Sun, "Absorption enhancement in double-sided nanocone hole arrays for solar cells," Journal of Optics, vol. 17, (7) pp. 1-6, 2015.

Absorption enhancement in double-sided nanocone hole arrays for solar cells

Xu Zhang[1, 2, *], Yanguang Yu[2], Jiangtao Xi[2], Yile Wang[1], Xiao-Hong Sun[1]

[1]Henan Key Laboratory of Laser and Opto-electric Information Technology, School of Information Engineering, Zhengzhou University, Zhengzhou, 450052, China

[2]School of Electrical, Computer and Telecommunications Engineering, University of Wollongong, Northfields Ave, Wollongong, NSW 2522, Australia

**zhangxubetter@gmail.com*

Abstract: Enhancing light absorption in thin-film silicon solar cells is important for improving light harvesting efficiency and reducing manufacture cost. In this paper, we introduce a double-sided nanocone hole array (NCH) structure for solar cells by extending a model suggested by Wang *et al*. [Nano Lett. **12**, 1616, (2012)]. The top-sided NCH structure is mainly used for increasing the antireflection of incident light, and the bottom-sided NCH structure for enhancing light trapping in the near-infrared spectrum. The theoretical analysis is performed on the proposed structure, from which the optimal geometric parameters of the structure are determined. The performance analysis shows that the proposed optimized double-sided NCH structure can yield a short-circuit current of 31.9 mA/cm^2 with equivalent thickness of 1μm, which is 12% and 190% higher than that of the top-sided NCH and planar film counterparts respectively.

Keywords: Photovoltaic, Subwavelength structure, Solar energy

1. Introduction

Solar photovoltaic (PV) technologies are gaining considerable interest as one set of the most promising solution to future fossil energy shortage and environmental pollution. In recent years, thin film silicon solar cells have attracted great interest for low-cost applications. Efficient light trapping scheme in a thin film requires good coupling of incident light, broadband antireflection and effective light trapping character. However, weak absorption, especially in the long wavelength that near the vicinity of silicon bandgap edge, remains a challenge. To address this problem, textured active layer into nanostructure array have been extensively studied, such as nanowire [1-3], nanocone [4-6], nanohole and nanocone hole (NCH) [7,8] arrays. Among these, NCH arrays have been demonstrated with a promising capabilities of harvesting sunlight over a large wavelength [7,8]. It has the following advantages over the other counterparts: (1) The properties of mechanical robustness due to the redistribution of the normal and shearing mechanical loads [9]; (2) For single nanocone hole with the same bottom area and height as nanowire, the surface area of nanocone hole is only half of nanowire, which minimizes surface recombination losses under an equal array density; (3) The fabrication of the structures is easy and cost-effective. The ordered NCH arrays are fabricated by a scalable multistep

anodization and wet etching process on an imprinted metal foil in an acidic solution [10]. The height and radii of NCH arrays could be controlled preciously in the fabrication process. Therefore, this technique provides a useful and practical way for the fabrication of NCH structure solar cells.

These advantages mentioned above suggest that NCH arrays are excellent structures for high efficiency thin film solar cells with reasonable robustness. In order to further increase the absorptance of NCH arrays, surface plasmonic effect in metallic structure deposited on the back of NCH textured film is regarded as one solution [11]. It will give rise to absorption increment in the long wavelength range, which contributes about 10% improvement to the total absorption [12]. Nevertheless, it will give rise to the parasitic absorption due to the metal-semiconductor contact [13]. To solve this problem, while making use of the light trapping effect of surface plasmonics, an alternative method is proposed. In this paper, we put forward a new architecture of double-sided NCH array solar cells by extending a nanocone model suggested by Wang *et al*. [Nano Lett. **12**, 1616, (2012)]. The top-sided NCH structure is mainly used for increasing the antireflection of incident light, while the bottom-sided NCH structure plays an important role in light trapping to achieve broadband absorption enhancement. Due to mechanical robustness and cost-effective fabrication process as compared to nanocone array [4-6], the proposed model possesses industrial manufacturing value.

The optimization method is as follow: first, for a give structure only patterned with top-sided NCH, by using rigorous coupled wave analysis (RCWA) [14,15], we calculate the integrated absorption from which the optimized geometric parameters of top-sided NCH structure, including the base period, height and radius of NCH arrays are determined. Second, we consider a double-sided NCH structure with the optimized top-sided NCH design. The absorption enhancement strategy in this hybrid structure design requires broad band absorption over the entire usable solar spectrum, especially the light trapping ability from 800 to 1100nm where the silicon is weakly absorbing. In this regard, the optimal period of bottom-sided NCH arrays should be close to the target wavelength[16,17]. Hence, the period of bottom-sided NCH arrays is chosen as 1μm by approximation. To determine the exact value, we should take into account the period of supercell (unit cell combined with both the top- and bottom-sided NCH) simultaneously, in order to reduce the simulation complexity. Finally, with the predetermined period of bottom-sided NCH arrays, the optimized geometric parameters of bottom-sided NCH arrays are obtained by utilizing the same calculation procedure as the first step. In this optimization, we adjust these geometric parameters, while ensuring the structure always consists of the same amount of silicon material as a planar thin film with fixed thickness of 1μm.

2. New structure and its optimal geometric parameters

2.1 Double-sided NCH structure

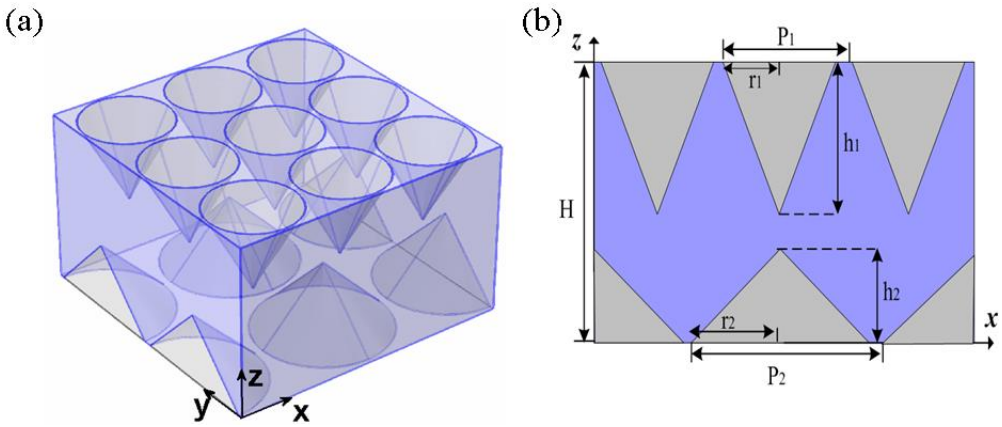

Fig. 1. (a) Schematic of a structure of the double-sided NCH textured silicon thin film layer. (b) The cross-section of NCH arrays in the *x*-*z* plane.

A schematic diagram of the proposed solar cell model is shown in Fig. 1(a) and its cross-section view in Fig. 1(b). It can be seen that the double-sided NCH arrays are arranged in a square lattice in the *x*-*y* plane and surrounded by air. The main parameters of the structure are represented by the periods (P_1 and P_2), heights (h_1 and h_2), and the radii (r_1 and r_2) of top and bottom-sided NCH arrays respectively. Then the filling factors, defined as the unit cell area occupied by hole on the surface area, are given by $F_1=\pi r_1^2/P_1^2$ and $F_2=\pi r_2^2/P_2^2$ for the top- and bottom-sided NCH arrays respectively. The structure is illuminated at normal incident sunlight with a wavelength range from 310 to 1100nm. The refractive index of silicon is taken from the literature [18].

2.2 Determine the optical geometric parameters

The RCWA algorithm is employed to calculated the integrated absorption *A* under an air mass AM1.5 incident solar irradiance. It is a semi-analytical method in computational electromagnetics that is most typically applied to solve scattering from periodic dielectric structures. Periodic boundary conditions are applied in the *x* and *y* directions. The accuracy of the solution depends only on the number of terms in the field space-harmonic expansion. In this paper, the simulation has been performed with 24 harmonics for each *x* and *y* axis. Then the integrated absorption in silicon can be readily obtained as

$$A = \int_0^{\lambda_g} \alpha(\lambda)\, I(\lambda) d(\lambda) \,/\, \int_0^{\infty} I(\lambda) d\lambda \tag{1}$$

where $I(\lambda)$ is the AM1.5G solar intensity [19], and λ_g is the wavelength corresponding to the bandgap, $\alpha(\lambda)$ is the absorption spectrum which can be expressed as

$$\alpha(\lambda) = \frac{\omega}{2} \varepsilon_0 \,\mathrm{Im}[\varepsilon_r(\omega)] \iiint |E(r,\omega)|^2 dV \tag{2}$$

where ω is the angular frequency of light, ε_0 and ε_r are the vacuum permittivity and relative permittivity of the material respectively, $E(r, \omega)$ is the electric field intensity, and V is the volume of the structure.

The maximum integrated absorption of top NCH arrays depends on the geometrical parameters, including the period, filling factor and height. We firstly optimize the period and filling factor with height h_1 equals 0.5μm. Then, the height will be further optimized in the following. It is theoretically possible to find the configuration that maximizes the integrated absorption by scanning simultaneously filling factor F_1 (between 0.3 and 0.7) and period P_1 (between 0.3 and 0.9μm). The result of this scan is depicted on the mapping in Fig. 2(a), where the integrated absorption is given as a function of F_1 and P_1. When the period is much smaller than the incident light wavelength, the optical diffraction is too weak to couple into the NCH textured silicon layer, resulting in a low absorption ratio. Hence, the maximum value of about 57% is reached for F_1=0.7 and P_1=0.7μm. The integrated absorption with optimized F_1 and P_1 as a function of height h_1 is shown in Fig. 2(b). The height varies from 0 to 900nm with a step of 90nm. One can see that integrated absorption increases with increasing height. The height of zero corresponds to the planar film layer, with absorption much smaller than the rest. It has almost reached saturation state when the height is larger than 0.6μm, and the maximum absorption value of 61% is observed. However, the surface area increases with height, that is to say, the electrical performance turns worse with the increasing height. Therefore, the optimized height value of 0.6μm is chosen. In this case, the surface area only increases by a factor of 1.8, which limits surface recombination losses in compared with other light trapping schemes. Thus the top-sided NCH textured silicon thin film layer achieves the maximum integrated absorption value of 57%, with F_1=0.7, P_1=0.7μm and h_1=0.6μm.

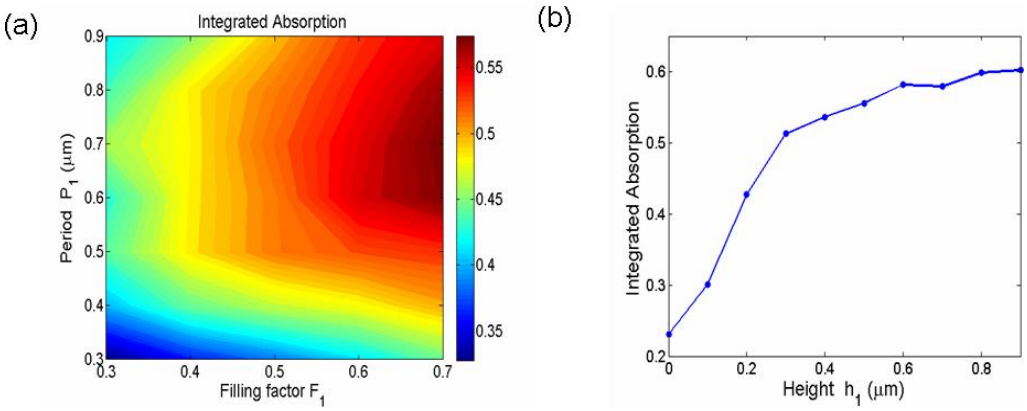

Fig. 2 (a) Contour map of the integrated absorption in the top-sided NCH arrays as a function of period and filling factor, and the AM1.5G solar spectral intensity distribution was taken into account. (b) The integrated absorption as a function of height.

Next we turn to the geometrical optimization of the bottom-sided NCH arrays. The light trapping ability of the proposed structure relies on the excitation of guided resonance modes [20,21], therefore a careful choice of period is important. For large period, more guide resonance modes would be excited, which leads to higher absorption. However, each of the excited resonance modes could not be coupled to many external channels, so the small period is preferable. Hence, the optimal period for light trapping should be on the wavelength order for scattering light

effectively[16,17]. For silicon, light trapping is important for the 800 to 1100nm wavelength range. In order to couple long wavelength light efficiently into the guided resonance modes, the optimal period of the bottom-sided NCH arrays is chosen as 1μm by approximation. To determine the exact value, we should take into account the period of supercell (unit cell combined with both the top- and bottom-sided NCH) simultaneously, just for reducing simulation complexity. As the optimal period of top-sided NCH is obtained (P_1=0.7μm), we need to find out the lowest common multiple of 0.7μm and ~1μm. From mathematic point of view, the periods of supercell and bottom-sided NCH arrays are chosen as 2.1μm and 1.05μm respectively. That means 9 top-sided NCHs and 4 bottom-sided NCHs are included in one supercell unit. As shown in Fig.3(a), the integrated absorption with optimized top-sided NCH array parameters are calculated for different filling factors F_2 and heights h_2. The maximum integrated absorption value of 62% is obtained for F_2=0.7 and height h_2=0.5μm at fixed P_2=1.05μm. The impact of bottom-sided NCH arrays on the absorption spectrum of solar cell model is presented in Fig.3(b). This figure demonstrates the absorptance spectrum of bottom-sided NCH arrays with period of 0.8μm, 0.9μm and 1.05μm respectively. We can see that in the short wavelength range (λ<0.8μm), there is a trivial difference between these three curves. However, as the wavelength beyond 0.8μm, the absorptance of bottom-sided NCH arrays with period of 1.05μm shows superiority over the others. This result verifies our previous expectation about optimal period for bottom-sided NCH arrays.

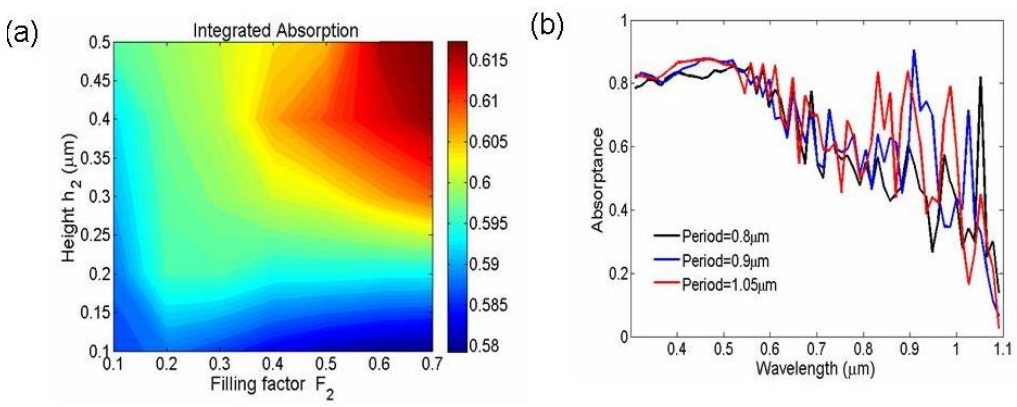

Fig. 3 (a) Contour map of the integrated absorption in the double-sided NCH arrays with optimized top-sided NCH array parameters as a function of filling factor F_2 and height h_2. (b) Absorptance of bottom-sided NCH array with period of 0.8μm, 0.9μm and 1.05μm respectively.

3. Performance analysis

3.1 The absorption enhancement and light trapping

The analysis above has obtained the optimized parameters for the double-sided NCH textured arrays. In order to determine the absorption enhancement factor of this hybrid nanostructure, the absorption ratio is calculated. It is defined as the ratio between the integrated absorption of the double-sided NCH textured arrays to the top-sided NCH textured arrays. It can be seen in Fig. 4 that as large as 6-fold

absorption enhancement is observed at the wavelength of 1020nm. And several peaks are observed in the absorption spectrum, which corresponds to different guided resonant modes. Owning to the large absorption coefficient of silicon in short wavelength, the incident light are almost nearly fully captured before they can reach the bottom-sided NCH arrays. As a result, virtually no light interact with the bottom area, which can explain the overlapped absorptance spectra of top and double-sided NCH textured arrays in the wavelength region smaller than 500nm in Fig. 6(a). However, as the increase of incident wavelength, the absorption coefficient of silicon keeps dropping, leading to the interaction between the incident light and bottom-sided NCH arrays.

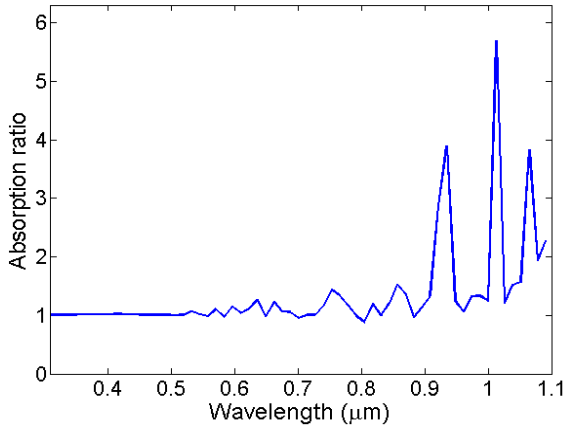

Fig. 4 Absorption ratio for the optimized double-sided NCH textured arrays.

To shed light on how light is coupled into the structure, the cross-section electric field intensity ($|E|^2$) distribution of the electromagnetic wave at the 400nm and 1000nm are plotted as demonstrated in Fig. 5, using finite element method (FEM) implemented in the RF module of COMSOL Multiphysics. The $|E|^2$ distribution is displayed in the *x*-*z* plane integrated over the a whole structure in *y* direction. Perfect magnetic and electric conductor (PMCs and PECs) are used on the sidewalls for generating either symmetric magnetic field or symmetric electric field. Periodic boundary conditions are applied in the *x* and *y* directions while perfect matched layer boundary conditions are used for the *z* direction. The maximum mesh size is chosen to be 40nm in air and 10nm in NCH structure for accurate calculation. Note that the color index at the specific location in the cross-section $|E|^2$ distribution indicates the magnitude of $|E|^2$ at that point, normalized with that of source wave propagating in free space.

As shown in Fig. 5, a structure with top-, bottom- and double-sided NCH array is labeled as (a, d), (b, e) and (c, f) respectively. From fig. 5(a, c), we can see that the top-sided NCH can suppresses surface reflection at the wavelength of 400nm, thus increase the absorption. At this short wavelength, light is mainly absorbed by the top structure, as it could not transmit too long in silicon. Therefore, the bottom-sided NCH array plays no significant role in the short wavelength absorption. Similar results can also be seen in fig. 5(b). At the wavelength of 1020nm, which corresponding to the sharp increase of absorptance in Fig.4, the bottom-sided NCH

arrays contribute dramatically to the absorption enhancement. The incident light goes deep into silicon, and the scattered field gives rise to diffraction for a periodic structure. A number of discrete electric field domains with strong intensity are spotted in Fig. 5(e). As demonstrated in Fig. 5(f), the strongest electric fields are distributed in the vicinity of top-sided NCH array, especially near the tip and double side area of NCH structure. With the contribution bottom-sided NCH arrays, the electric field intensity of double-sided structure gets more stronger than only top-sided NCH arrays, especially in the long wavelength range.

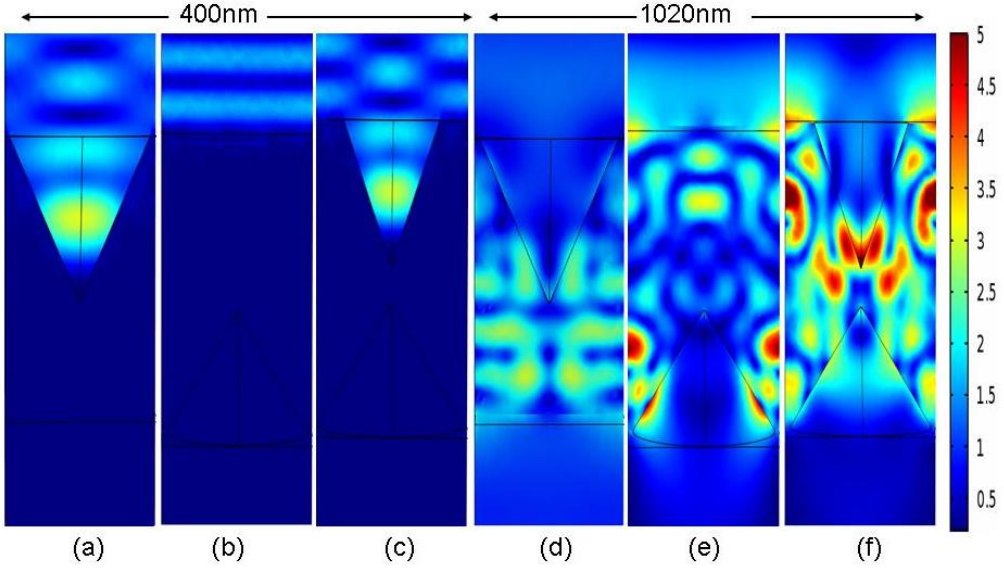

Fig. 5 The electric field intensity profiles at wavelength of (a)-(c) 400nm and (d)-(f) 1000nm for top-sided (a) and (d) NCH arrays, (b) and (e) bottom-sided NCH arrays, (c) and (f) double-sided NCH arrays respectively.

3.2 Short-circuit current comparison

In Fig. 6(a), we compare the performance of our proposed structure to the top-sided NCH arrays, planar silicon film and Yablonovitch limit with the same equivalent thickness of 1μm. Assuming perfect antireflection and light trapping property, the absorption spectrum in a thin film with thickness of d is given by the Yablonovitch limit [22-24]

$$A_{Yablonovitch} = 1 - \frac{1}{1 + 4n^2 \alpha d} \tag{3}$$

where α is the absorption coefficient and n is the real part of the refractive index.

To evaluate the absorption capability of our proposed solar cell structure, we calculate the short-circuit current, which is given by [25]

$$J_{sc} = \frac{e}{hc} \int \lambda I(\lambda) \alpha(\lambda) d\lambda \tag{4}$$

where e is the elementary charge, h is Planck's constant, c is the speed of light. When using Eq. (4), all the generated charge carriers are assumed to be collected and contribute to the photocurrent without considering the effect of recombination losses. Comparing the absorption spectrum of our optimized design structure to that of planar

thin film in Fig. 6(a), a substantial absorption enhancement over the entire wavelength range is observed, which originates mainly from antireflection. It is due to a gradual refractive index change, the light reflection from the air and NCH textured interface is substantially suppressed. However, there is little difference between top- and double-sided NCH arrays in the short wavelength range. Meanwhile, in the long wavelength region, the absorptance of double-sided NCH arrays exceeds the Yablonovitch limit, which is mainly contributed from the bottom-sided NCH arrays. Fig. 6(b) illustrates the short-circuit currents for double- (I), top- (II) sided NCH arrays, planar film layer(III) and the Yablonovitch limit (red dotted line). The short-circuit current of 31.9 mA/cm^2 is achieved for double-sided NCH structure, which is 12% and 190% higher than that of the top-sided and planar film counterparts respectively.

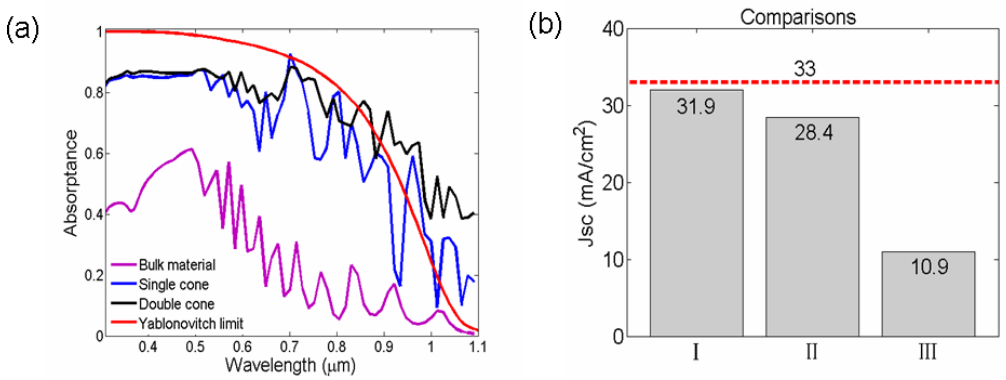

Fig. 6(a) Absorptance of the optimized double-sided NCH arrays compared to that of top-sided NCH arrays and planar film counterparts. (b) The short-circuit current for double- (I), top- (II) sided NCH arrays, planar film(III) as well as the Yablonovitch limit (red dotted line).

Conclusions

To summarize, the absorption properties of double-sided NCH arrays for solar cells are demonstrated. The top-sided NCH structure is mainly used for increasing the antireflection of incident light, while the bottom-sided NCH structure plays an important role in light trapping to achieve broadband absorption enhancement. The results show that the proposed structure with the optimized geometric configuration can greatly enhance the absorption in the whole wavelength range. The short-circuit current of 31.9 mA/cm^2 is achieved with an equivalent thickness of 1μm, which is 12% and 190% higher than that of the top-sided and planar film counterparts respectively. Overall, the proposed structure provides a promising way to improve the absorption of silicon thin film solar cells.

Acknowledgments

This work was supported by the Foundation Research Project of Henan Province (No. 132300410072), Foundation of Henan Educational Committee (No. 14B510015), and National Natural Science Foundation of China (11104251).

References

1. Kelzenberg M D, Boettcher S W, Petykiewicz J A, Turner-Evans D B, Putnam M C, Warren E L, Spurgeon J M, Briggs R M, Lewis N S and Atwater H A 2010 Enhanced absorption and carrier collection in Si wire array for photovoltaic applications *Nat. Mater*. **9 239–244**
2. Chang H, Lai K, Dai Y, Wang H, Lin C and He J 2011 Nanowire arrays with controlled structure profiles for maximizing optical collection efficiency *Energy Environ. Sci*. **4 2863–2869**
3. Shin J C, Kim K H, Yu K J, Hu H, Yin L, Ning C, Rogers J A, Zuo J and Li X 2011 In(x)Ga(1-x)as nanowires on silicon: one-dimensional heterogeneous epitaxy, bandgap engineering and photovoltaics *Nano Lett.* **11 4831–4838**
4. Wang K X, Yu Z F, Liu V, Cui Y and Fan S H 2012 Absorption enhancement in ultrathin crystalline silicon solar cells with antireflection and light-trapping nanocone gratings *Nano Lett.* **12 1616–1619**
5. Jeong S, Garnett E C, Wang S, Yu Z, Fan S, Brongersma M L, McGehee M D and Cui Y 2012 Hybrid silicon nanocone-polymer solar cells *Nano Lett.* **12 2971–2976**
6. Wang B and Leu P W 2012 Enhanced absorption in silicon nanocone arrays for photovoltaics *Nanotechnology* **23 194003**
7. Wang W, Zhang J, Zhang Y, Xie Z, and Qin G G 2013 Optical absorption enhancement in submicrometre crystalline silicon films with nanotexturing arrays for solar photovoltaic applications *J. Phys. D: Appl. Phys.* **46 195106**
8. Xie Z, Wang W, Qin L, Xu W and Qin G G 2013 Optical absorption characteristics of nanometer and submicron a-Si:H solar cells with two kinds of nano textures *Opt. Express* **21 18043**
9. Kim J, Choi H J, Park K, Cohen R E, McKinley G H and Barbastathis G 2014 Multifunctional inverted nanocone arrays for non-wetting, self-cleaning transparent surface with high mechanical robustness *Small* **10 2487-94**
10. Lin Q F, Leung S F, Lu L F, Chen X Y, Chen Z, Tang H N, Su W J, Li D D and Fan Z Y 2014 Inverted nanocone-based thin film photovoltaics with omnidirectionally enhanced performance *ACS Nano*. **8 6484**
11. Zhang X, Yu Y G, Xi J T, Liu T L and Sun X H 2015 The plasmonic enhancement in silicon nanocone hole solar cells with back located metal particles *Journal of Optics* **17 015901**
12. Chen Y K, Han W H and Yang F H 2013 Enhanced optical absorption in nanohole-textured silicon thin-film solar cells with rear-located metal particles *Opt. Lett.* **38 3973-3975**
13. Yahaya N A, Yamada N, Kotaki Y and Nakayama T 2012 Characterization of light absorption in thin-film silicon with periodic nanohole arrays *Opt. Express* **21 5924–30**
14. Moharam M G, Pommet D A, and Grann E B 1995 Stable implementation of the rigorous coupled-wave analysis for surface-relief gratings: enhanced transmittance matrix approach *J. Opt. Soc. Am. A* **12 1077**
15. Moharam M G, Grann E B, Pommet D A and Gaylord T K 1995 Formulation for stable and efficient implementation of the rigorous coupled-wave analysis of binary gratings *J. Opt. Soc. Am. A* **12 1068**

16. Yu Z, Raman A and Fan S 2010 Fundamental limit of light trapping in grating structure *Opt. Express* **18 A366**
17. Yu Z, Raman A and Fan S 2010 Fundamental limit of nanophotonic light trapping in solar cells *Proc. Natl. Acad. Sci. U.S.A.* **107 17491-17496**
18. Palik E. D 1985 Handbook of Optical Constants of Solids Vol. 5 (Orlando: Academic).
19. Pala R A, White J, Barnard E, Liu J and Brongersma M L 2009 Design of plasmonic thin-film solar cells with broad band absorption enhancements *Adv. Mater.* **21 3504**
20. Zhang X, Sun X H, Huang H, Wang X S, Huang Y Q and Ren X M 2014 Optical absorption in InP/InGaAs/InP double-heterostructure nanopillar arrays for solar cells *Appl. Phys. Lett.* **104 061110**
21. Zhang X, Sun X H and Jiang L D 2013 Absorption enhancement using nanoneedle array for solar cell *Appl. Phys. Lett.* **103 211110**
22. Yablonovitch E 1982 Statistical ray optics *J. Opt. Soc. Am.* **72 899−907**
23. Yablonovitch E and Cody G D 1982 Intensity enhancement in textured optical sheets for solar cells *IEEE Trans. Electron Devices* **29 300−305**
24. Green M A 2002 Lambertian light trapping in textured solar cells and light-emitting diodes: analytical solutions *Prog. Photovoltaics* **10 235−241**
25. Lin C and Povinelli M L 2009 Optical absorption enhancement in silicon nanowire arrays with a large lattice constant for photovoltaic applications *Opt. Express* **17 19371**